DOI 10.31489/2021Ph3/115-121
UDC 544.14

T.M. Serikov*, A.E. Sadykova, P.A. Zhanbirbayeva, A.S. Baltabekov, A.S. Kayumova

Karagandy University of the name of academician E.A. Buketov, Kazakhstan
*(*E-mail: Serikov-timur@mail.ru)*

Photocatalytic water splitting of nanocomposite materials based on TiO_2 and rGO nanorods

The paper presents the results of a study of films formed by titanium dioxide nanorods and deposited on their surface of reduced graphene oxide by electrochemical deposition. Nanostructured films based on TiO_2 nanorods were prepared in a 100 ml stainless steel autoclave with a fluoroplastic insert from a solution containing 35 ml of deionized water (H_2O), 35 ml of hydrochloric acid (HCl) (36.5 %, Sigma–Aldrich) and 0.25 ml of titanium butylate $C_{16}H_{36}O_4Ti$ (97 %, Sigma–Aldrich). The addition of reduced graphene oxide to the structure of titanium dioxide nanorods increases the specific surface area of nanostructures from 29.3 m^2/g to 63.1 m^2/g. Calculations based on the film impedance spectra have shown that the optimal deposition time of reduced graphene oxide on the surface of TiO_2 nanorods is 3 minutes, since it has a low recombination coefficient and a long electron lifetime. Studies of the photocatalytic activity of nanomaterials and registration of the released hydrogen and oxygen gases have shown that when the films are irradiated for 5 hours, the amount of hydrogen released varies from 50 to 225 $mmol/cm^2$.

Keywords: nanorods, graphene oxide, specific surface area, photo-splitting of water.

Introduction

Hydrogen is practically not found on Earth in its pure form and must be extracted from other compounds using various chemical methods. According to the source [1], 75 million tons of hydrogen are consumed annually in the world. Moreover, three-quarters of it is carried out by steam conversion of methane and natural gas, and this consumes about 205 billion m^3 of gas. Almost everything else is obtained from coal and only 0.1 % (~100 thousand tons) is extracted by splitting water by electrolysis or in photoelectrochemical cells and solar thermochemical systems. Sunlight can be used to directly produce hydrogen from water using modern photoelectrochemical, thermochemical, and photobiological processes. Direct use of sunlight is the most efficient way to produce hydrogen, as it avoids energy losses. According to the European Commission, the main investors in the development of hydrogen energy were the United States (~$500 million), Japan (~$300 million) and the EU countries (~$230 million). The leading countries also include South Korea (~$100 million) and China (~$60 million). In the future, the main regions for fuel cell sales are India, China, and Africa, where the development of the telecommunications market is largely constrained by an imperfect power supply system. In the countries of the former USSR, including Kazakhstan, investments in the development of hydrogen energy are very small. Therefore, conducting fundamental research that will generate new scientific information can contribute to the development of hydrogen production technologies in our country.

In the process of photodegradation of water, there is a need to create highly efficient photocatalysts that can absorb solar radiation and divide the water molecule into hydrogen gas and oxygen.

For effective photocatalytic splitting of water, photocatalysts are used, the band gap of which should cover the oxidation potentials of water, which are +0 and +1.23 V with respect to the normal hydrogen electrode (NHE) at pH= 0. Such photocatalysts include wide-band semiconductors such as ZrO_2, ZnO, TiO_2, WO_3 [2, 3], perovskite materials of the composition $CaTi_{0.98}Cu_{0.02}O_3$, Rh/Ta/F: $SrTiO_3$, Cr/Ta/F: $SrTiO_3$, etc. [4].

Among the listed photocatalysts, titanium dioxide (TiO_2) occupies a special place due to its physical, optical, electrical and photocatalytic properties. Using various synthetic approaches, it is possible to obtain zero-dimensional, one-dimensional and two-dimensional nanostructures of titanium dioxide [5–7]. Its one-dimensional formations, such as nanorods, have a number of advantages over zero-dimensional and two-dimensional ones. 3–dimensional electron transport is carried out in films made of TiO_2 nanoparticles. The features of agglomeration of dioxide nanoparticles during thermal annealing significantly affect the possibilities of electronic transitions between them. Non-intensive chemical binding leads to a decrease in the efficiency of electron transport. In view of this, when using TiO_2 nanorods in the process of photocatalytic decomposition of water, it is possible to expect a preferential transport of electrons along their walls, which

will reduce the transfer time from the charge carrier generation centers to the chemical reaction boundary, and also, when optimizing the design will allow to achieve a smaller number of surface defects. In addition, TiO_2 nanorods in controlled synthesis may have a higher specific surface area than spherical nanoparticles. However, a significant disadvantage of TiO_2 nanorods is its wide band gap (about 3.2 eV), which indicates the absorption band only in the ultraviolet region of the electromagnetic wave. Increasing the sensitivity of such films in the visible region can be achieved by using hybrid nanostructures, for example, in combination with graphene. To date, graphene (a monatomic layer of graphite) nanostructures are promising materials for use in photovoltaics, electronics, photocatalytic water splitting and in systems for cleaning from organic pollutants [8–11]. Grapheme is optically transparent, chemically functional, has a high mobility of charge carriers and the value of the specific surface area. The production of graphene nanostructures is well studied and it can be easily obtained by the well-known Hammer method [12]. In practice, graphene oxide is often synthesized. However, for the transport of electrons through the material, it is necessary to restore the sp^2 aromatic structure of graphene oxide, which results in reduced graphene oxide. Often, recovery occurs by chemical, photochemical, and hydrothermal methods [13–15]. The use of graphene nanostructures in semiconductor films made of titanium dioxide nanorods will improve the separation of electron-hole pairs, increase the absorption capacity of semiconductor films in the visible region of the electromagnetic wave, and lead to an increase in the specific surface area of nanostructures as a whole. These factors are expected to significantly improve the photocatalytic activity of the films.

Experimental

Nanostructured films based on TiO_2 nanorods were prepared in a stainless steel autoclave with a fluoroplastic insert. A solution containing 15 ml of deionized water, 15 ml of HCl (36.5 %, No. 320331, Sigma–Aldrich) and 0.25 ml of titanium butylate $C_{16}H_{36}O_4Ti$ (97 %, No. 244112, Sigma–Aldrich) was poured into a 50 ml fluoroplast insert. TiO_2 nanorods were synthesized on FTO substrates (7 ohms/cm^2, No. 735167, Sigma–Aldrich), previously purified by ultrasound treatment in a mixture of deionized water, acetone and 2-propanol (volume ratio 1 : 1 : 1) for 30 min. The prepared FTO substrates were then placed in the autoclave with the conductive side down. The temperature treatment was carried out in a convective furnace (8,2/1100, SNOL). The furnace temperature and the synthesis duration are 200 ^{0}C in the range from 100 ^{0}C to 200 ^{0}C and from 6 to 24 hours, respectively. The resulting samples were washed with deionized water and dried at room temperature. The samples were then calcined at a temperature of 500 ^{0}C for 2 hours in air.

Further, to obtain the NR TiO_2/rGO composite material, commercial rGO powder (Reduced Graphen Oxide, Cheaptubes Inc.) was delaminated in 0.1 M pH 9.32. phosphate buffer solution (PBS, Na_2HPO_4, and NaH_2PO_4) and treated in an ultrasonic bath for 90 min to form a brown colloidal RGO dispersion with a concentration of 0.5 mg/ml. The deposition was carried out using a three-electrode system (HC TiO_2 as the working electrode, Pt foil as the counter electrode, and Ag/AgCl electrode as the reference electrode) at the ELINS electrochemical plant (R-20XV, Russia). The number of graphene oxide sheets deposited was controlled by a deposition time of 1 to 15 minutes. After precipitation the NR TiO_2/rGO composite material was washed with ethylene glycol and deionized water and then dried at room temperature.

Images of the sample surface were obtained using a scanning electron microscope (SEM) (MIRA 3 LMU, Tescan). The voltage at the accelerating electrode was 20 keV.

Spectrophotometric measurements were carried out on an automatic scanning spectrophotometer Solar CM 2203 (Solar) in the wavelength range of 250–800 nm with a spectral resolution of 0.5 nm.

The textural characteristics of synthesized samples were calculated on the basis of nitrogen adsorption and desorption isotherms at a temperature of 77K obtained at the quantachrome volumetric unit («Sorbi», USA). The specific surface area of the samples was estimated by the Brunauer-Emmett–Taylor method (BET).

A photoelectrochemical cell was used to record the released hydrogen. The cell window is quartz (Minihua Store). The opposite electrode is platinum. The solutions were separated using a Nafion filter. Nanostructures of titanium dioxide and graphene oxide were used as the working electrode. Both sides of the cell were pre-purged with a stream of argon gas. Then, when the sample was irradiated, samples were taken and identified on an Agilent gas chromatograph (Lomonosov Moscow State University).

Based on the obtained impedance spectra for the films the electrophysical parameters of the Z-500PRO impedance meter (Elins, Russia) were calculated when irradiated with a xenon lamp with a power of 100 MW/cm^2. The amplitude of the applied signal was up to 25 mV, and the frequency range was from 1 MHz to 100 MHz. Platinum coatings used as the opposite electrode were deposited from an ethanol solution of H2PtCl6 by electrochemical method on glass substrates with a conductive layer of FTO. The electrodes were

glued together. A polymer film Meltonix (Solaronix, Switzerland) with a thickness of 25 microns served as a spacer between the working electrode and the removal electrode in the solar cell.

Results and discussions

Figure 1 shows the surface morphology of NR TiO_2 films. As can be seen from the figure, before the deposition of graphene oxide nanolayers, the film consists of titanium dioxide nanorods. The average length of the nanorods disoriented with respect to the substrate surface in this case was ~120 nm and the average diameter ~ 43 nm (Fig. 1a).

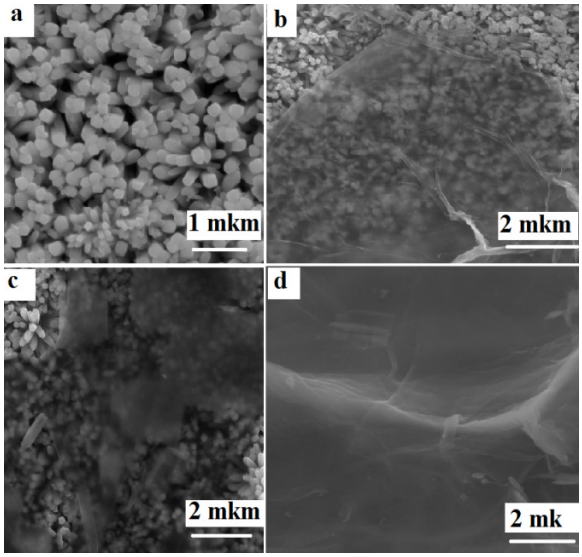

A-clean; b-1 min.; c-3 min.; d-5 min..

Figure 1. SEM images of the NR TiO_2/rGO nanocomposite

When the deposition time is about 1 minute, graphene oxide sheets are formed on the surface of the NR. Graphene oxide is dispersed over the entire surface of the TiO_2 NR, which can form a conducting network between them. With an increase in the duration of the deposition process to 3 and 5 minutes, the number of deposited sheets increases, and with a 5 minute deposition the surface is completely covered with graphene oxide flakes. This will allow the TiO_2 NR to inject its photogenerated electrons into the graphene oxide sheets under the action of light, ensuring their efficient transport to the FTO layer and further registration of the photocurrent.

The study of the specific surface area of nanocomposite materials was carried out by the method of low-temperature nitrogen adsorption. To do this, the nanocomposite material is separated from the substrate. If necessary, the process was repeated until sufficient mass was obtained to change its specific surface area. The samples were thermotrained at a temperature of 95^0C for 180 minutes in the «SorbiPrep» pretreatment unit with a constant flow of adsorbate gas at a speed of 2 l/min. The measurement was carried out at a liquid nitrogen temperature of 77 K. Nitrogen was used as an adsorbate. Table 1 shows the dynamics of measuring the specific surface area of nanocomposite materials of the composition NR TiO_2/rGO as a function of the electrochemical deposition time.

Table 1

Specific surface area of nanocomposite materials of the composition NR TiO_2/rGO and NT TiO_2/rGO

№	Sample	Specific surface area S_{BET}, m^2/g	Full pore volume Vp, cm^3/g
1	rGO	600	0.416
2	NR TiO_2	29,3	0,165
3	NR TiO_2/ rGO_1 min	45,1	0,213
4	NR TiO_2/ rGO_3 min	52,8	0,231
5	NR TiO_2/ rGO_5 min	63,1	0,249

From the presented data it can be seen that the addition of TiO2/mgo to the HC structure significantly increases the specific surface area of the nanostructures. Thus, for HC films the specific area before the deposition of graphene oxide was 29.3 m^2/g, after which it increased to 63.1 m^2/g, as well as the volume of the adsorbed gas.

The nitrogen adsorption-desorption isotherms for all samples have the same appearance, except for the volume of adsorbed nitrogen. At low relative pressures (P/P_0 less than 0.1) an increase in nitrogen adsorption is observed on the isotherms, which indicates the presence of micropores. With an increase in the relative partial pressure for the samples, the volume of adsorbed nitrogen increases. In accordance with the IUPAC nomenclature, the obtained isotherms belong to the type IV isotherms with a hysteresis loop, reflecting the process of capillary condensation in mesopores.

The electric transport properties of nanocomposite materials were studied by the method of impedance spectroscopy. From the central arc of the impedance spectra, the effective recombination rate keff, the effective electron lifetime teff, the electron transport resistance in titanium dioxide films Rw, and the charge transfer resistance Rk associated with electron recombination were calculated according to the above method. Figure 2 shows the hodographs in Nyquist coordinates for the synthesized samples.

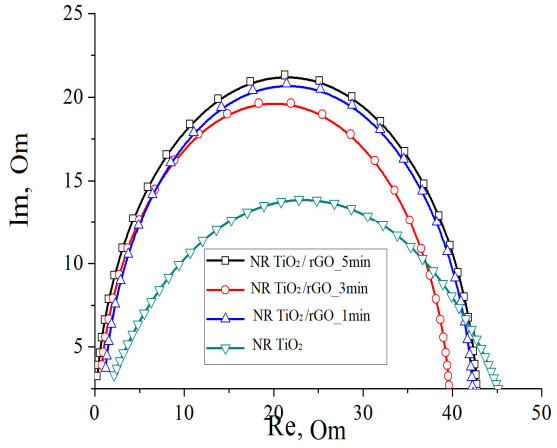

Figure 2. Impedance spectra of nanocomposite materials

The electron transport resistance in the nanocomposite R_w and the charge transfer resistance R_k will depend directly on the number of electrons received from the number of free electrons. If we take into account that the size and thickness of the semiconductor film are identical for all systems only the deposited layers of graphene oxide will affect the resistance value. The brief calculations are presented in Table 2.

Table 2

Electric transport properties of films based on nanocomposite materials

Sample	k_{eff}, c^{-1}	τ_{eff}, c	R_k. Om	R_w, Om
NR TiO_2	15	0,06	45	3
NR TiO_2/ rGO_1 min	12	0,08	42	2
NR TiO_2/ rGO_3 min	11	0,09	39	2
NR TiO_2/ rGO_5 min	14	0,07	41	2

The method allows us to calculate the main electric transport properties of nanocomposite films. However, a number of conclusions can be drawn from the results obtained. From the tabular data it can be seen that in the TiO_2 / mgo_3 min NR a low recombination coefficient and a long electron lifetime are observed. This indirectly indicates that in these cells the recovery of the electrolyte at the electrolyte/catalyst interface (graphene oxide) is more efficient than in the others.

The edge of the absorption spectrum of HC TiO_2 appears in the UV region of the spectrum around 380 nm. RGO also absorbs in the UV zone, the maximum of its absorption spectrum is at 230 nm. At the same time, the RGO film is almost transparent in the wavelength range from 400 to 800 nm. SiO_2-GO nanocomposites also actively absorb light in the UV region of the spectrum. Along with this, there is a broadening of the absorption band in the visible range of the spectrum.

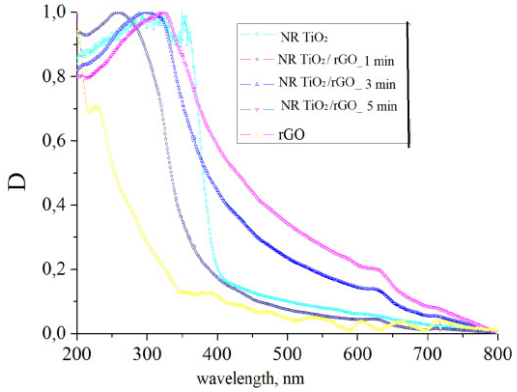

Figure 3. Absorption spectra of a nanocomposite of the composition NR TiO_2/rGO

Next, the photocatalytic activity of nanomaterials was investigated. The results of the experiments are shown in Figure 3.

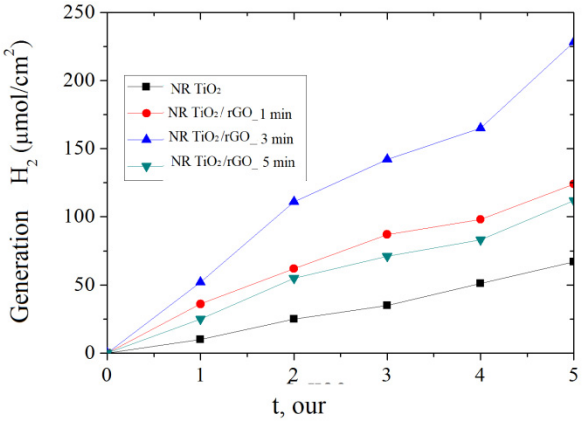

Figure 4. Photocatalytic cleavage of NR TiO_2/rGO water

From the presented data it can be seen that the addition of TiO_2 to the HC structures in various concentrations leads to an increase in their photocatalytic activity and water splitting. Moreover, it is necessary to determine the optimal concentration of graphene oxide. In this case, the best generation of hydrogen is observed by electrochemical deposition within 3 minutes, compared to other nanocomposite layers.

Conclusion

Electrochemically, sheets of reduced graphene oxide were deposited on the surface of the TiO_2 NR at a deposition time of 1, 3, and 5 minutes. The influence of the preparation conditions of nanostructured materials on their specific surface area, structure, electrophysical, optical and photocatalytic properties is investigated. The addition of TiO_2 rGO to the NR structure significantly increases the specific surface area of the nanostructures. Thus, for NR films the specific area before the deposition of graphene oxide was 29.3 m^2/g, after which it increased to 63.1 m^2/g, as well as the volume of the adsorbed gas. Low recombination coefficient and long electron lifetime are observed in films made of HC TiO_2 / rGO 3 min.

References

1 Serikov T.M. The effect of electric transport properties of titanium dioxide nanostructures on their photocatalytic activity / T.M. Serikov // Bulletin of the university of Karaganda. — Physics. — 2020. — № 3. — P. 13–21.

2 Kang Z Interface Engineering for Modulation of Charge Carrier Behavior in ZnO Photoelectrochemical Water Splitting / H. Kang, Z, Si, S. Zhang // Advanced functional materials. — 2019. — № 29. — P. 15.

3 Zhai K., Li K., Zhu X. Oxygen Exchange Materials Used in Two-Steps Thermochemical Water Splitting for Hydrogen Production / K. Zhai, K. Li, X. Zhu // Progress in chemistry. — 2015. — № 27, T 10. — P. 1481–1499.

4 Muhamad A. Titanate-based perovskites for photochemical and photoelectrochemical water splitting applications: A review / A. Muhamad, A. Khuzaimah, J. Lorna // International journal of hydrogen energy. — 2018. — № 43. — P. 23209–23220.

5 Fujishima A. Electrochemical photolysis of water at a semiconductor electrode / A. Fujishima, K. Honda // Nature. — 1972. — Vol. 238. — P. 37–38.

6 Pereira L. UV/TiO_2 Photocatalytic Degradation of Xanthene Dyes / L. Pereira, R. Pereira, K.S. Oliveira, L. Apostol // Photochemistry and Photobiology. — 2013. — Vol. 89. — P. 33–39.

7 Akinobu M. Water Splitting on Rutile TiO_2-Based Photocatalysts / M. Akinobu, N. Shunta // Chemistry A European Journal. — 2018. — № 24. — P. 204–219.

8 Kamat P.V. Graphene-based nanoassemblies for energy conversion / P.V. Kamat // The Journal of Physical Chemistry Letters. — 2010. — № 2. — P. 242 — 251.

9 Wang D.H. Self-assembled TiO_2-graphene hybrid nanostructures for enhanced Li-Ion insertion / D.H. Wang, D.W. Choi, J. Li, Z.G. Yang, Z.M. Nie, R. Kou, et al. // ACS Nano. — 2009. — № 3. — P. 907–914.

10 Wang X. Transparent, Conductive graphene electrodes for dye-sensitized solar cells / X. Wang, L. Zhi, K. Muellen // Nano Letters. — 2008. — № 8. — P. 323–327.

11 Serp P. *Carbon Materials for Catalysis* / P. Serp, J.L. Figueiredo, etc. — Hoboken, N.J.: John Wiley & Sons, 2009.

12 Hummers Jr W.S. Preparation of graphitic oxide / Jr W.S. Hummers, R.E. Offeman // Journal of the American Chemical Society. — 1958. — № 80. — P. 1339.

13 Li D. Processable aqueous dispersions of graphene nanosheets / D. Li, M.B. Muller, S. Gilje, R.B. Kaner, G.G. Wallace // Nature Nanotechnology. — 2008. — № 3. — P. 101–105.

14 Williams G. TiO2-graphene nanocomposites. UV-assisted photocatalytic reduction of graphene oxide / G.Williams, B. Seger, P.V. Kamat // ACS Nano. — 2008. — № 2. — P. 1487–1491.

15 Zhou Y. Hydrothermal dehydration for the «green» reduction of exfoliated graphene oxide to graphene and demonstration of tunable optical limiting properties / Y. Zhou, Q.L. Bao, L.A.L. Tang, Y.L. Zhong, K.P. Loh // Chemistry of Materials. — 2009. — № 21. — P. 2950–2956.

Т.М. Сериков, А.Е. Садыкова, П.А. Жанбирбаева, А.С. Балтабеков, А.С. Каюмова

TiO_2 және rGO негізіндегі нанокомпозитті материалдарда фотокатализ арқылы суды ыдырату

Мақалада титан диоксиді наноөзекшелері және оның бетіне электрохимиялық әдісімен тұндырылған графен оксидінен қалыптасқан қабыршақтарды зерттеу нәтижелері келтірілген. TiO_2 наноөзекшелері негізінде жасалған нанокұрылымды қабыршақтар көлемі 100 мл тот баспайтын болаттан және фторопласттан жасалған автоклав ішінде синтезделеді. Автоклавтың ішіне 35 мл ионсыздандырылған су (H_2O), 35 мл тұз қышқылы (HCl) (36,5 %, Sigma-Aldrich) және 0,25 мл титан бутилатының $C_{16}H_{36}O_4Ti$ (97 %, Sigma–Aldrich) қосындысы бар сұйықтық дайындалады. Титан диоксиді наноөзекшелерінің құрамына графен оксидін қосу, нанокұрылымдардың меншікті бетінің аумағын 29,3 $м^2$/ г-нан 63,1 $м^2$ / г-ға дейін арттырады. Қабыршақтардың импеданс спектрлерін қолдана отырып, жүргізілген есептеулер TiO_2 наноөзекшелерінің бетіне графен оксидінің оңтайлы тұндыру уақыты 3 минутты құрайтындығын көрсетті, себебі оның рекомбинация коэффициенті өзге үлгілерге қарағанда төмен және электрондардың өмір сүру уақыты жоғары. Наноматериалдардың фотокаталитикалық белсенділігі мен сутегі және оттегінің бөлінген газдарын тіркелу барысында, қабыршақтарды 5 сағат сәулелендіру кезінде бөлінетін сутектің мөлшері 50-ден 225 ммоль / $см^2$-ге дейін өзгеретінін көрсетті.

Кілт сөздер: наностержень, графен оксиді, беттік аудан, судың фотоыдырауы.

Т.М. Сериков, А.Е. Садыкова, П.А. Жанбирбаева, А.С. Балтабеков, А.С. Каюмова

Фотокаталитическое расщепление воды нанокомпозитных материалов на основе наностержней TiO_2 и rGO

Представлены результаты исследования пленок, образованных наностержнями диоксида титана и осажденных на их поверхность восстановленного оксида графена, методом электрохимического осаждения. Наноструктурированные пленки на основе наностержней TiO_2 получали в автоклаве из нержавеющей стали с фторопластовой вставкой объемом 100 мл из раствора, содержащего 35 мл деионизованной воды (H_2O), 35 мл соляной кислоты (HCl) (36,5 %, Sigma–Aldrich) и 0,25 мл бутилата титана $C_{16}H_{36}O_4Ti$ (97 %, Sigma–Aldrich). Добавление в структуру наностержней диоксида титана восстановленного оксида графена увеличивает удельную площадь поверхности наноструктур от 29,3 $м^2$/г до 63,1 $м^2$/г. Проведенные расчеты по спектрам импеданса пленок показали, что оптимальное время осаждения восстановленного оксида графена на поверхность наностержней TiO_2 составляет 3 мин, так как для него наблюдается низкий коэффициент рекомбинации и длительное время жизни электронов. Исследования фотокаталитической активности наноматериалов и регистрация выделяемых газов во-

дорода и кислорода показали, что при облучении пленок в течение 5 ч количество выделяемого водорода варьируется от 50 до 225 ммоль/см^2.

Ключевые слова: наностержень, оксид графена, удельная поверхность, фоторасщепление воды, облучение.

References

1 Serikov, T.M. (2020). The effect of electric transport properties of titanium dioxide nanostructures on their photocatalytic activity. *Bulletin of the university of Karaganda. Physics, 3,* 13–21.

2 Kang, Z, Si H., & Zhang, S. (2019). Interface Engineering for Modulation of Charge Carrier Behavior in ZnO Photoelectrochemical Water Splitting. *Advanced functional materials, 29,* P.15.

3 Zhai, K., Li, K., & Zhu, X. (2015). Oxygen Exchange Materials Used in Two-Steps Thermochemical Water Splitting for Hydrogen Production. *Progress in chemistry, 27(10),* 1481–1499.

4 Muhamad, A., Khuzaimah, A., & Lorna, J. (2018). Titanate-based perovskites for photochemical and photoelectrochemical water splitting applications: A review. *International journal of hydrogen energy, 43,* 23209–23220.

5 Fujishima, A., & Honda, K. (1972). Electrochemical photolysis of water at a semiconductor electrode. *Nature, 238,* 37–38.

6 Pereira, L., Pereira, R., Oliveira, K.S., & Apostol, L. (2013). UV/TiO_2 Photocatalytic Degradation of Xanthene Dyes. *Photochemistry and Photobiology, 89,* 33–39.

7 Akinobu, M., & Shunta, N. (2018). Water Splitting on Rutile TiO2-Based Photocatalysts. *Chemistry A European Journal, 24,* 204–219.

8 Kamat, P.V. (2010). Graphene-based nanoassemblies for energy conversion. *The Journal of Physical Chemistry Letters*, 2, 242–251.

9 Wang, D.H., Choi, D.W., Li, J., Yang, Z.G., Nie, Z.M., Kou, R., et al. (2009). Self-assembled TiO_2-graphene hybrid nanostructures for enhanced Li-Ion insertion. *ACS Nano*, 3, 907–914.

10 Wang, X., Zhi, L., & Muellen, K. (2008). Transparent, Conductive graphene electrodes for dye-sensitized solar cells. *Nano Letters*, 8, 323–327.

11 Serp, P., & Figueiredo, J.L. (2009). *Carbon Materials for Catalysis*. Hoboken, N.J.: John Wiley & Sons.

12 Hummers, Jr W.S., & Offeman, R.E. (1958). Preparation of graphitic oxide. Journal of the American Chemical Society, 80, 1339.

13 Li, D., Muller, M.B., Gilje, S., Kaner, R.B., & Wallace, G.G. (2008). Processable aqueous dispersions of graphene nanosheets. *Nature Nanotechnology, 3,* 101–105.

14 Williams, G., Seger, B., & Kamat, P.V. (2008). TiO_2-graphene nanocomposites. UV-assisted photocatalytic reduction of graphene oxide. ACS Nano, 2. 1487 — 1491.

15 Zhou, Y., Bao, Q.L., Tang, L.A.L., Zhong, Y.L., & Loh, K.P. (2009). Hydrothermal dehydration for the «green» reduction of exfoliated graphene oxide to graphene and demonstration of tunable optical limiting properties. Chemistry of Materials, 21, 2950–2956.